REPORT DOCUMENTATION PAGE

AFRL-SR-BL-TR-99-

0289

Public reporting burden for this collection of information is estimated to average 1 hour per response, including the time for review gathering and maintaining the data needed, and completing and reviewing the collection of information. Send comments regardi of information, including suggestions for reducing this burden to Washington Headquarters Service, Directorate for Information O 1215 Jefferson Davis Highway, Suite 1204, Arlington, VA 22202-4302, and to the Office of Management and Budget, Paperwork Reduction Project (0704-0188) Washington, DC 20503.

PLEASE DO NOT RETURN YOUR FORM TO THE ABOVE ADDRESS.

1. REPORT DATE *(DD-MM-YYYY)* 12/10/99	2. REPORT DATE October 22, 1999	3. DATES COVERED *(From - To)* June 1995–Nov. 1999

4. TITLE AND SUBTITLE Photonics and Nonlinear Optics with Molecular and Polymeric Materials	5a. CONTRACT NUMBER
	5b. GRANT NUMBER F49620-95-1-0412
	5c. PROGRAM ELEMENT NUMBER

6. AUTHOR(S) Dr. Paras N. Prasad	5d. PROJECT NUMBER
	5e. TASK NUMBER
	5f. WORK UNIT NUMBER

7. PERFORMING ORGANIZATION NAME(S) AND ADDRESS(ES) The Research Foundation of SUNY on behalf of State University of New York at Buffalo PO Box 9 Albany, NY 12201	8. PERFORMING ORGANIZATION REPORT NUMBER

9. SPONSORING/MONITORING AGENCY NAME(S) AND ADDRESS(ES) Air Force Office of Scientific Research 110 Ducnan Avenu, Suite B115 Bolling AFB, DC 20332	10. SPONSOR/MONITOR'S ACRONYM(S) AFOSR
	11. SPONSORING/MONITORING AGENCY REPORT NUMBER

12. DISTRIBUTION AVAILABILITY STATEMENT

Unlimited

13. SUPPLEMENTARY NOTES

14. ABSTRACT

See attached

19991215 091

15. SUBJECT TERMS

16. SECURITY CLASSIFICATION OF:			17. LIMITATION OF ABSTRACT	18. NUMBER OF PAGES	19a. NAME OF RESPONSIBLE PERSON Dr. Paras Prasad
a. REPORT	b. ABSTRACT	c. THIS PAGE			19b. TELEPONE NUMBER *(Include area code)* 716:645-6800 (x2098)
U	U	U	UU	12	

Standard Form 298 (Rev. 8-98)
Prescribed by ANSI-Std Z39-18

DTIC QUALITY INSPECTED 3

FINAL PROGRESS REPORT

PROJECT: Photonics and Nonlinear Optics with Molecular and Polymeric Materials

PERIOD: June 1, 1995 to November 30, 1998

SPONSOR: DOD Ballistic Missile Defense Organization/ Air Force Office of Scientific Research

CONTRACT NO: F49620-95-10412

PRICIPAL INVESTIGATOR: Dr. Paras N. Prasad

Photonics Research Laboratory

Department of Chemistry

State University of New York

Buffalo. New York 14260-3000

ABSTRACT

The work under this AASERT grant focused on the development of novel photonics materials. The emphasis was on the preparation of nanoscale composites, which in the bulk form are of high optical quality. A major focus is to prepare organic:inorganic nanocomposites. Er doped glasses are widely used for amplification and lasing at 1.5 μm. We have successfully prepared Er^{3+} doped multicomponent sol gel glasses with an objective to use them as amplifiers. IR lasers and upconversion lasers. They show enhanced radiative properties and strong upconversion.

The ability to use semiconductor nanocrystals as a sensitizer in an otherwise entirely organic photorefractive composite has been demonstrated. Furthermore, the figures of merit associated with this composite (PVK:TCP:NPP:CdS NCs) are of sufficient magnitude to qualify this composite as a "high-gain material". In addition to the validation of this approach, we have also achieved, for the first time, the photorefractive effect in a polymeric composite at 1310 nm, demonstrating the technological merits of this approach.

Er^{3+} multicomponent sol gel silica glass:

Silica glass is a highly attractive matrix for optical applications due to its favorable thermal and mechanical properties[1]. Rare earth doped silica glasses are potential materials for solid state fiber lasers, amplifiers[2] and upconversion lasers[3]. There have been several attempts to make Er-doped glasses by the sol-gel method for optical applications. However, the success was severely restricted by the fact that the rare earth ions have a tendency to have a nonuniform distribution and form clusters in the bulk, which reduce the fluorescence efficiency and lifetime. The presence of a large concentration of hydroxyl groups in the sol-gel glasses also degrades the emission properties. In order to prepare device quality silica glasses doped with rare earth ions, the hydroxyl quenching and ion clustering must be eliminated. A process has been developed to make multicomponent sol gel silica glasses with a low hydroxyl concentration and uniform distribution of rare earth ions.

A study of the hydroxyl concentration was performed for several Er^{3+} doped sol gel samples. Figure 1 shows the hydroxyl concentration that varied from 1200 ppm to 56 ppm for the Er doped sol gel and the Er multicomponent sol gel respectively. The multicomponent glass also shows an increased UV transmission and a decreased baseline, as shown in figure 2.
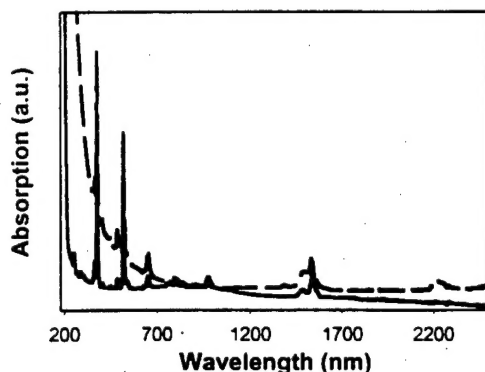

Figure 1. Uv-vis absorption spectra. The solid line represents the Er doped multicomponent sol gel glass. The dashed line represents the Er doped sol gel glass.
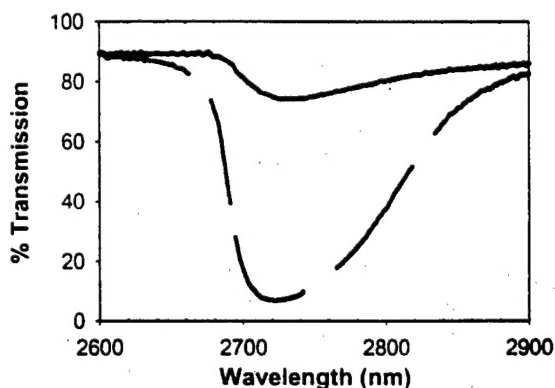
Figure 2. Hydroxyl concentration determination by NIR transmission. The solid line represents the Er doped multicomponent sol gel glass. The dashed line represents the Er doped sol gel glass.

The upconversion of rare earth ions strongly depends on their surrounding environment. The upconverted emission of the multicomponent glass is ~30 times greater than the simple Er doped sol gel, as shown in figure 3. The relative intensity of the upconverted fluorescence at 530 nm decreases as the upconverted fluorescence at 549 nm increases for the multicomponent sol gel. This is expected to be a result of the decreased phonon energy of the multicomponent glass.

The infrared fluorescence spectra of the samples in the wavelength range 1400-1700 nm are shown in figure 4. Er-doped glass shows a peak at 1534 nm that shifted to 1540 nm in the case of the multicomponent sample with enhanced linewidth and intensity. The peak emission is about 100 times more intense than that from the simple Er doped sol gel glass.
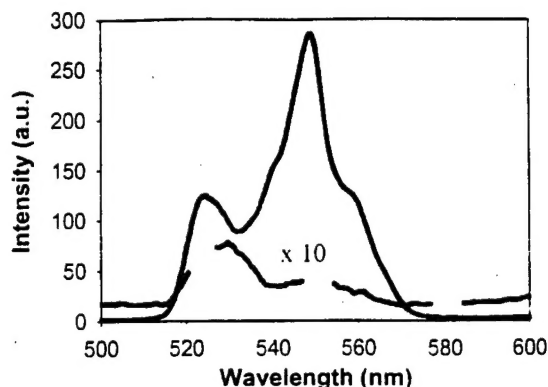
Figure 3. Upconverted fluorescence. The solid line represents the Er doped multicomponent sol gel glass. The dashed line represents the Er doped sol gel glass. The Er doped sol gel spectra has been magnified 10 times.
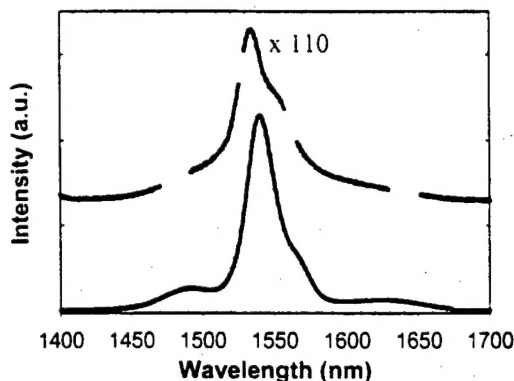
Figure 4. IR Fluorescence. The solid line represents the Er doped multicomponent sol gel glass. The dashed line represents the Er doped sol gel glass. The Er doped sol gel spectra has been magnified 110 times. The baseline has been shifted for easier viewing.

Due to the greatly enhanced properties of the multicomponent glass the calculated gain at 1.5 μm has been calculated. This glass is expected to achieve 5.4 dB/cm, which is better than the reported values of 4 and 1 dB/cm for phosphate and sol gel waveguides respectively. This data is presented in table 1.

Sample	Phosphate (waveguide) [4]	Phosphate (fiber) [5]	Si-TiO$_2$-Al-Yb-Er: sol-gel (waveguide) [6]	Silica-Al (fiber) [7]	Fluoride (fiber) [8]	Sol-gel processed multi-component silica glass (bulk)
Gain (dB/cm)	4.1	2.1	1	1	0.0075*	5.4**
λ_{pump} (μm)	0.98	0.98	0.98	0.98	1.48	0.98
P$_{pump}$ (mW)	27	110	160	250	113	Not estimated
λ_{signal} (μm)	1.535	1.537	1.532	1.533	1.58	1.54
Fluorescence lifetime (ms)	Not given	7.9 (bulk)	8.5	9.6	Not given	12.1
[Er^{3+}]	5.3 x 10^{19} cm^{-3}	3.7 x 10^{20} cm^{-3}	1.1 x 10^{20} cm^{-3}	1.6 x 10^{20} cm^{-3}	1310 ppm	1.6 x 10^{20} cm^{-3}

Table 1. Comparison of spectral properties of various Er doped glasses.

Thus, the multicomponent glass has a clear edge over the untreated glass in reducing both the hydroxyl concentration and rare earth clustering. This has reduced the quenching observed in Er-doped sol-gel glasses. These glasses are optically transparent and light pink in color. Further studies will focus on lasing action at 1.5 μm and upconversion lasing.

Observation of the Photorefractive Effect in a Hybrid Organic-Inorganic Nanocomposite:

Introduction

The realization of advanced information and image processing technology depends on the development of multifunctional materials which are able to simultaneously satisfy several requirements.[9, 10] One such technology involves the photorefractive effect. Photorefractivity in polymeric systems, considered to be potential media for high density optical data storage, optical amplification, and dynamic image processing, is an area of considerable regard where major achievements have been made.[11-17]

Polymeric composites exhibiting the photorefractive effect are especially attractive when compared with their inorganic counterparts for many reasons, including their relative ease of preparation, inexpensive commercial availability, design flexibility, and low dielectric constant. Despite the promising characteristics affiliated with polymeric photorefractive materials, several deficiencies are still associated with these composites. The application of a relatively large electric field in order to obtain an acceptable photorefractive figure-of-merit has proven to be a major hurdle. Also, while there are several polymers known to show reasonable charge generation in the ultraviolet region, it is often desirable to enhance their optical response in the visible and infrared regions. It was originally believed that the ability to dope these materials with different organic dyes for the purposes of spectral sensitization would lead to the ability to tune the spectral response of these composites. This speculation was met, however, with limited success. While there are many such dyes, few are known to exhibit sufficient charge generation quantum efficiency Φ to be considered for practical application and, to our knowledge, none have been reported which can be utilized to photosensitize these photorefractive polymeric composites at 1.31 or 1.55 μm, wavelengths commonly used in data-storage and telecommunications. In an effort to address the need for high electric fields as well as the spectral limitations encountered with conventional organic dyes, we have developed a novel approach to the sensitization of photoconductive polymer matrices (photoconductivity is a necessary component of the photorefractive effect) with inorganic semiconducting nanocrystals (NCs).

Semiconductor nanocrystallites are a potentially useful class of photosensitizers capable of fast and efficient charge generation. Due to this increased efficiency, relative to traditional organic sensitizers, the magnitude of the electric field required to elicit a photoelectric response is significantly reduced. Also, due to the unique physical properties identified with these NCs, the spectral limitations associated with organic sensitizers may be overcome through this novel approach. As the reduction in size of a semiconductor NC surpasses a certain critical limit, the band-gap, or difference in energy between the highest occupied molecular orbit (HOMO) and that of the lowest unoccupied molecular orbit (LUMO), will begin to increase. This shift in the band-gap translates into the ability to control the absorption characteristics (and hence, the spectral response) of the final product through the appropriate choice of NC size as well as composition. Doping of photoconductive or photorefractive polymers with only a few weight percent of semiconductor NCs leads to a new class of organic-inorganic hybrid composites with charge generation capabilities which have been shown to exceed those previously reported for traditional organic sensitizers.[18] Since the concentration of the NCs lies below their percolation threshold, they are effectively isolated and responsible for charge-generation while the polymer matrix is responsible for charge-transport.

We report here on the use of inorganic semiconductor NCs as photosensitizers in an otherwise entirely organic composite. The NC photosensitizers employed in this study are cadmium sulfide and lead sulfide. The surfaces of the NCs have been passivated with an organic layer consisting of p-thiocresol, effectively preventing the agglomeration of the NCs. This organic passivating layer also renders the surface of the NC hydrophobic, enabling the incorporation of the inorganic NCs into an organic environment.

In all cases, poly-vinyl carbazole (PVK), a prototypical hole-conducting polymer, acts as the charge transporting matrix. Electro-optic modulation of the refractive index, a necessary component of the photorefractive effect, is accomplished though the inclusion of the chromophore nitrophenyl L-prolinol (NPP). The introduction of tricresyl phosphate (TCP), an inert plasticizing agent, sufficiently lowers the glass-transition temperature T_g of the composite to allow for room temperature poling of the second-order nonlinear electro-optic chromophores.

Experimental
a. Synthesis of Semiconductor Nanocrystals

The syntheses used in this study are based on methods which have come to be firmly established in the literature. these methods can be divided into two main categories: i) the first in which the final size of the NC is governed by the ratio of sulfide concentration to thiol concentration employed during the synthetic operation, and ii) the second, in which the crystal size is dictated by the size of the micellar cavity in which the crystal is grown.

i) In the first method, described as competitive reaction chemistry (CRC),[19] the mechanism of cluster formation has been termed as an inorganic form of polymerization. In the initiation phase of the synthesis a solution containing metal ions (cadmium or lead in this case), generated from the respective acetate, is introduced into a solution containing S^{2-} and RS^-, in the form of sodium sulfide and p-thiocresol respectively, in order to create sub-nanoparticles of CdS or PbS. Once formed, a propagation step in which the particles aggregate competes with the growth terminating reaction of the thiolate with the surface of the NC.[11] It has also been shown that although being covalently bonded to the surface of semiconductor NCs, the thiocresol species is dislocated by additional sulfide ions allowing for further growth of the cluster. However, once a sulfide ion has been incorporated into a given cluster, it can not be replaced by a thiolate ion.[11] Through this process the NCs are allowed to grow until the supply of S^{2-} has been exhausted.

A detailed synthesis for CdS (S^{2-}:RS^- = 1:0.2) employing the CRC method is as follows: sodium sulfide (0.8 g, 10 mmol) and p-thiocresol (0.25 g, 2 mmol) were dissolved in 50 ml water, 50 ml methanol and 100 ml acetonitrile, vigorously stirred and purged with nitrogen for 15 minutes. To this solution was added dropwise cadmium acetate dihydrate (5.34 g, 20 mmol) dissolved in a mixture of methanol and acetonitrile (4:1 ratio), yielding an opaque orange dispersion. This dispersion was evaporated to dryness and the product was washed exhaustively with methanol.

ii) The second method involves the use of reverse micelles (RM) as microreactors to obtain organically encapsulated nanoparticles. The reverse micellar system is generally composed of two immiscible liquids (water and oil) where the aqueous phase is dispersed as nanosize water droplets encapsulated by a monolayer film of surfactant molecules in a continuous nonpolar organic solvent such as a hydrocarbon. In this study the continuous oil phase consists of isooctane and sodium bis(2-ethylhexyl)sulfosuccinate (AOT) serves as the surfactant. In addition to water, aqueous solutions containing a variety of dissolved salts, including cadmium acetate, lead acetate, and sodium sulfide can be solubilized within the reverse micelles.[20] The size of the micelle, and subsequently the volume of the aqueous pool contained within the micelle, is governed by the water to surfactant ratio, also termed W_0, where $W_0 = [H_2O]/[surfactant]$.[21] Continuous exchange of the micellar contents through dynamic collisions enables the reaction to proceed. However, since the reaction is confined within the cavity of the micelle, growth of the particle beyond the dimensions of the cavity is inhibited. In the final stage of this synthesis, the passivating reagent, p-thiocresol, is added to the continuous oil phase. This species is then able to enter the aqueous phase as RS^- and bond to the surface of the contained particle, eventually rendering the surface of the particle hydrophobic and thereby inducing precipitation of the capped NC.

A detailed account of the RM synthesis of CdS NCs ($W_0 = 10$) is as follows: two solutions of sodium bis(2-ethylhexyl) sulfosuccinate (8.9 g, 20 mmol) in 200 ml n-heptane were prepared. To one of these solutions was added cadmium acetate dihydrate (96 mg, 0.36 mmol) in 3.6 ml water and to the other was added sodium sulfide (28 mg, 0.36 mmol) in 3.6 ml water. These two solutions were simultaneously poured into a single vessel producing a non-scattering yellow dispersion, followed by the immediate introduction of p-thiocresol (0.28 g, 3.6 mmol) in 36 ml heptane. After stirring the reaction mixture for 24 hours, the precipitated surface capped CdS was collected through filtration and washed with methanol.

Both methods of NC preparation presented yield a free flowing powder and were easily redispersed in several organic solvents such as pyridine, dimethyl formamide, and cyclopentanone, allowing for optical characterization of the solvated product as well as doping of a polymer (PVK) matrix to form an inorganic-organic composite system. Significant optical scattering by the NCs was not observed, permitting their use in applications requiring samples of high optical quality (e.g., photorefractivity).

b. Fabrication of Samples

CdS or PbS was first dispersed in pyridine followed by subsequent introduction of PVK, TCP, and NPP, where the weight percent composition of PVK:TCP:NPP:NC is represented by the ratio 53.5:40.13:5.35:1.01. The filtered dispersion (0.2 μm pore size membrane) was cast on ITO coated glass substrates with an etched electrode pattern. The films were allowed to dry at ambient conditions for 24 hours and subsequently heated to 70° C in a vacuum oven for 24 hours to ensure complete solvent evaporation. Next, two films were softened by placing them on a hot plate (200° C) for 30 seconds and pressed together to produce a sandwich glass-ITO-polymer-ITO-glass arrangement between the etched

ITO-coated substrates yielding samples which were 100 - 200 μm in thickness. The T_g of the composite was determined to fall below 14 °C, the lower detection limit of the employed differential scanning calorimeter. The film preparation was performed in a class 100 cleanroom.

c. Photorefractive Characterizations

The photorefractive properties of the PVK:NPP:TCP:NC composite samples were studied via two wave mixing and degenerate four wave mixing techniques using an oblique experimental setup. In the case of samples containing CdS, characterizations were performed using an Ar⁻ laser operating at 514.5 nm and for samples containing PbS, a diode laser emitting at 1310 nm was employed. Holographic gratings were written through the intersection of two coherent beams with s-polarization in the FWM experiment and p-polarization in the TWM experiment. The two writing beams, (I_1) and (I_2), intersected in the sample with incident angles of $\theta_1 = 60°$ and $\theta_2 = 38°$ (in air) respectively. In the DFWM experiment, a p-polarized reading beam (I_r) propagated in a direction opposite to one of the writing beams (I_1). In the TWM experiments, the asymmetric energy transfer between the p-polarized writing beams was observed by monitoring the intensity of each of the writing beams by two photodetectors when an external electric field was applied. All data were digitized using a digital multimeter and transferred to a computer. For steady state conditions, the data were collected for a period of 30 s and averaged.

Results

This section will be divided into two main divisions, in the first, the results pertaining to the CdS NC composite will be presented. This will be followed by a presentation of the results pertaining to the PbS NC composite.

a. CdS Nanocrystal Composite

The electric field dependence of the photorefractive DFWM steady state diffraction efficiency obtained in a sample with a thickness of 146 μm is presented in figure 5. The maximum obtained steady state diffraction efficiency, η_{ssp}, is 8% at $E_0 = 137$ V/μm.
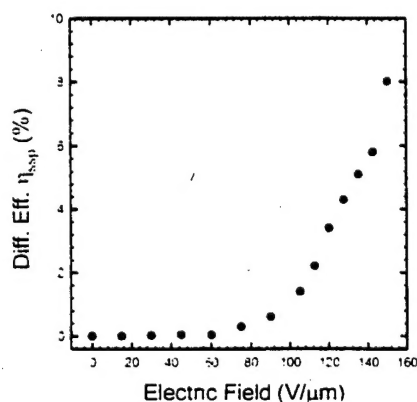

Figure 5. Photorefractive DFWM steady-state diffraction efficiency obtained in the CdS:PVK:TCP:NPP nanocmposite.
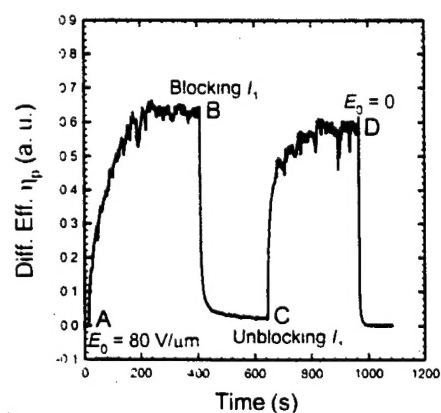
Figure 6. Diffraction efficiency as a function of time in the CdS:PVK:TCP:NPP nanocmposite.

Figure 6 depicts the diffraction efficiency as a function of time with a sample thickness of 169 μm. Two writing beams are turned on at time $t = 0$ followed by the subsequent application of an external electric

field ($E_0 = 80$ V/μm) at $t = 15$ s depicted as point A in fig. 6. at which time a rapid rise in the diffraction efficiency is observed. At
the point depicted as point B ($t = 408.5$ s) in fig. 6. the writing beam I_1 is blocked which results in relatively uniform illumination of the sample. leading to the erasure of the photorefractive grating. This ultimately causes a rapid decrease in the diffraction efficiency. At point C ($t = 646$ s) the blocked writing beam. I_1, is unblocked. allowing the PR grating to again achieve a steady state. At point D ($t = 968$ s) the external electric field is turned off. which allows for the random reorientation of the chromophores. leading to the erasure of the PR grating. The characteristic growth time. τ. can be determined using the equation.

$$\eta_p(t) \approx [E_{sc}(1-e^{-t/\tau})]^2.$$ 1.

where E_{sc} is the saturation value of the space-charge field.[29] A value of τ = 7.3 s was calculated for the sample by fitting the data represented between points C and D in fig. 13 to equation 2. In addition to demonstrating the temporal characteristics of the photorefractive grating written in this composite. this figure also serves to illustrate the possibility to record and erase PR gratings repeatedly in this composite.

A characteristic feature of the photorefractive effect is that the refractive index grating created in the medium is spatially shifted with respect to the light intensity pattern of the writing beams.[22,23] As a result an asymmetric energy transfer between beams interfering in a photorefractive sample occurs. Figure 3 depicts the data obtained in the TWM portion of the experiment to verify intensity exchange between laser beams and quantify the TWM gain coefficient for the PVK:TCP:NPP:CdS nanocomposite. For this experiment an external dc electric field $E_0 = 107$ V/μm was applied to a 168 μm thick sample at time $t = 70$ s and turned off at $t = 190$ s. The TWM coupling gain coefficient Γ is given in terms of the experimentally measured quantities γ_0 and β. as.

$$\Gamma = \frac{1}{L}[\ln(\gamma_0\beta) - \ln(\beta + 1 - \gamma_0)]$$ 2.

where L length of the optical path through the sample of the beam experiencing gain.β is of the writing beam intensities before the sample. and γ_0 is the beam-coupling ratio. defined as.

$$\gamma_0 = \frac{P_1}{P_0}$$ 3.

where P_1 is the intensity of the signal with the pump, and P_0 is the signal with out the pump.[22-26] A TWM gain coefficient of Γ = 39.5 cm^{-1} for writing beams with p-polarization at 514.5 nm was calculated for the data depicted in the figure. however: it is noted that when the sample was subjected to an external electric field of 119 V/μm. a TWM gain coefficient of Γ = 59.5 cm was measured just prior to the sample experiencing dielectric breakdown. From a practical point of view. the optical amplification. Γ, must exceed the absorption loss. α. of the photorefractive sample in question.[27] In this case the optical absorption of the sandwiched sample (glass/ITO polymer composite/ITO/glass) at 514.5 nm was measured to be α = 8.7 cm^{-1}. yielding a net gain coefficient. Γ - α. of 30.8 cm^{-1} at 107 V/μm and 50.8 cm^{-1} at 119 V/μm.
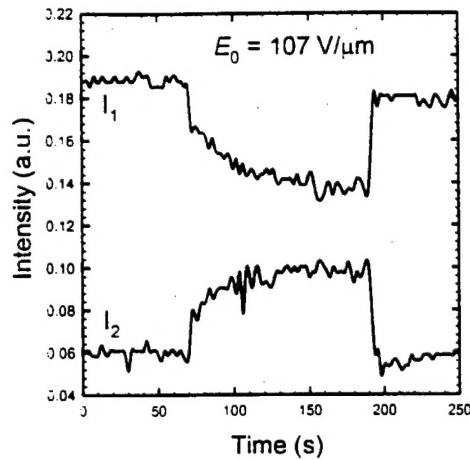
Figure 7. TWM for the CdS:PVK:TCP:NPP nanocmposite.

b. PbS Nanocrystal Composite

In the case of the PVK:TCP:NPP:PbS nanocomposite. DFWM characterizations have not yet been performed, however; the photorefractive capabilities of this composite have been demonstrated by way of TWM characterizations. As was the case with the PVK:TCP:NPP:CdS nanocomposite, the asymmetric energy transfer between two interfering laser beam arms ($\lambda = 1310$ μm) was monitored. Figure 8 depicts the data collected for this nanocomposite.
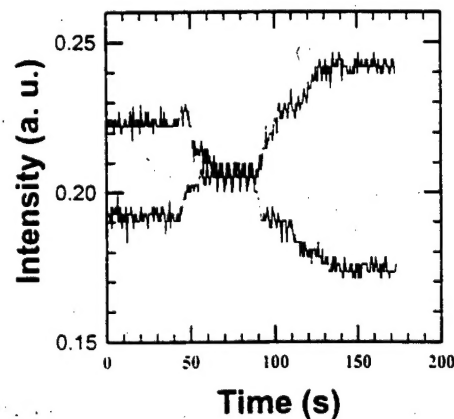

Figure 8. TWM for the PbS:PVK:TCP:NPP nanocmposite.

In this instance. $E_0 = 37$ V/μm. and $\Gamma = 16$ cm^{-1}. Just prior to dielectric breakdown. (<50 V/μm) a two beam coupling coefficient approaching $\Gamma = 30$ cm^{-1} was measured. which is comparable to values associated with state-of-art inorganic crystals. For this photorefractive sample. the absorption loss was

determined to be $\alpha = 4.6$ cm^{-1}, yielding a net gain coefficient, $\Gamma - \alpha$, of 32 cm^{-1} at 37 V/μm and 25 cm^{-1} at 50 V/μm. Thus the photorefractive effect has been demonstrated in polymeric composite for the first time at the technologically important wavelength of 1310 nm.

Conclusion

The ability to use semiconductor nanocrystals as a sensitizer in an otherwise entirely organic photorefractive composite has been demonstrated. Furthermore, the figures of merit associated with this composite (PVK:TCP:NPP:CdS NCs) are of sufficient magnitude to qualify this composite as a "high-gain material". In addition to the validation of this approach, we have also demonstrated, for the first time, the photorefractive effect in a polymeric composite at 1310 nm, demonstrating the technological merits of this approach.

References:

1   E.J.A. Pope and J.D. Mackenzie. J. Non-Cryst. Solids 106 (1988) 236.

2   M.J. Weber. J. Non-Cryst. Solids 123 (1990) 208.

3   See for example. *Rare-Earth Doped Fiber Lasers and Amplifiers*. edited by M. J. Digonnet (Dekker. New York. 1993), and references therein.

4   Yan et al.. Appl. Phys. Lett. 71. 2922 (1997).

5   Hwang et al.. Electron. Lett. 35, 1007 (1999).

6   Yeatman et al.. Opt. Commun. 164, 19 (1999).

7   De Barros et al.. IEEE Photon. Tech. Lett. 8, 761 (1996).

8   Ono et al.. Electron. Lett. 33, 1471 (1997).

9   Klein. L. C.. Ed. Photonics and Nonlinear Optics with Sol-Gel Processed Inorganic Glass: Organic Polymer Composite: Chapter 19. Kluwer Acedemic: Boston. (1994).

10   Mark. J. E.. Lee. C. Y. C.. Bianoni. P. A.. Eds. Hybrid Organic-Inorganic Composites. ACS Symposium Series 585. Chapter 25. Washington. (1995).

11   Moerner. W. E.; Silence. S. M. Chem. Rev. 94 127 (1994).

12   Kippelen, B.; Marder. S. R.; Hendrickx. E.; Maldonado. J. L.; Guillemet. G.; Volodin, B. L.; Steele. D. D.; Sandalphon, Y. Enami: Yao. Y. J.; Wang, J. F.; Rockel. H.: Erskine. L.; Peyghambarian. N. Science 279. 54 (1998).

13   Hendrickx. E.: Herlocker. J.; Maldonado. J. L.; Guillemet. G.; Rockel. H.; Erskine. L.; Marder, S. R.; Kippelen, B.; Peyghambarian. N. Proc. SPIE-Int. Soc. Opt. Eng. 3281, 268 (1998).

14   Prasad, P. N.; Cui, Y.; Swedek, B.; Cheng, N.; Kim, K. S. J. Phys. Chem. B. 101, 3530 (1997).

15   Zhang, Y.; Burzynski, R.; Ghoshal, S.; Casstevens, M.K. Adv. Mat. 8, 111 (1996).

16   Wang, Q.; Gharavi, A.: Li. W.; Yu, L. Polym. Prepr. (Am. Chem. Soc., Div. Polym. Chem.), 38, 516 (1997).

17   Peng, Z.: Gharavi. A. R.: Yu. L. J. Am. Chem. Soc. 119. 4622 (1997).

18   JPC paper

19   Herron, N.: Wang, Y.: Eckert. H. J. Amer. Chem. Soc. 112. 1322 (1990).

20   Masui, T.: Fujiwara. K.: Machida. K.: Adachi, G.: Sakata. T.: Mori, H. Chem. Mater. 9, 2197 (1997).

21   Pileni, M. P. J. Phys. Chem. 97, 6961 (1993).

22   Prasad, P. N.: Cui. Y.: Swedek, B.; Cheng, N.; Kim. K. S. J. Phys. Chem. B. 101, 3530 (1997).

23   Swedek. B.: Cheng, N.: Cui. Y.; Zieba. J.: Winiarz. J.: Prasad. P. N. J. Appl. Phys. 82. 5923 (1997).

24   Wang, Y. Pure and Appl. Chem. 68, 1475 (1996).

25   Yeh. P. IEEE. J. Quan. Electronic. 25. 484 (1989).

26   Donckers. M. C. J. M.; Silence, S. M.: Walsh. C. A.: Hache. F.: Burland, D. M.; Moerner. W. E.; Tweig, R. J. Opt. Lett. 18. 1044 (1993).

27   Nosaka, Y.: Yamaguchi. K.; Miyama. H.; Hayashi. H. Chem. Lett. 605 (1988).